

## Supporting Information

### **Electronic and Structural Programming via Electrochemical Dealloying to Generate Bi-Pb Electrocatalysts for CO<sub>2</sub> Reduction to Formate**

Samina Farid,<sup>\*a</sup> Ashi Rashid<sup>a,b</sup> Khurram Saleem Joya<sup>\*a,c</sup> and Farhat Yasmeen<sup>a</sup>

<sup>a</sup>Department of Chemistry, University of Engineering and Technology, GT Road 54890 Lahore, Pakistan,

<sup>b</sup>University of Leeds, Leeds, LS2 9JT, UK

<sup>c</sup>Department of Chemistry, Faculty of Science, Islamic University of Madinah, Madinah 42351, Saudi Arabia

\*Emails: (SF) [samina.farid117@gmail.com](mailto:samina.farid117@gmail.com); (KSJ) [khurram.joya@gmail.com](mailto:khurram.joya@gmail.com)

## Materials and Chemicals

Bi, Pb, and Sn foil (99.99%, 0.2 mm thickness) of analytical grade were obtained from Sigma-Aldrich. All the chemicals were used without any further purification. HCl (99.98%), HNO<sub>3</sub> (99.98%) H<sub>2</sub>SO<sub>4</sub> (99.98%) KHCO<sub>3</sub> (99.99%), C<sub>2</sub>H<sub>5</sub>OH (99.99%), (CH<sub>3</sub>)<sub>2</sub>CO (99.99%), NaCOOH (99.99%) were purchased from Sigma-Aldrich. CO<sub>2</sub> gas (99.998% purity) was obtained from reputed gas company, Lahore, Pakistan.

### ICP-OES (Inductively Coupled Plasma Optical Emission Spectroscopy) analysis

The bulk elemental content and composition (Pb, Bi, Sn) of prepared samples were determined using ICP-OES. For sample preparation, alloy foil crushed into fine powder using a mechanical grinder. The concentrated solution was prepared by dissolving metals in concentrated HNO<sub>3</sub> by constantly heating until all the particles completely dissolved. After that solution was diluted with ultrapure water to a suitable volume for ICP-OES analysis. The certified reference material of Pb, Bi, Sn was prepared for standard calibration at various concentrations (1ppm, 5ppm, 10ppm, 20ppm). The weight percentage (wt/%) was calculated from ppm concentration using dilution factor and mass of sample (mg). Here's the formula:

$$(Weight\ percentage\ (wt/\%)) = \frac{concentration\ (ppm) \times Dilution\ Factor}{Sample\ mass\ (mg)} \times 100$$

(1)

## Synthesis of electrodes

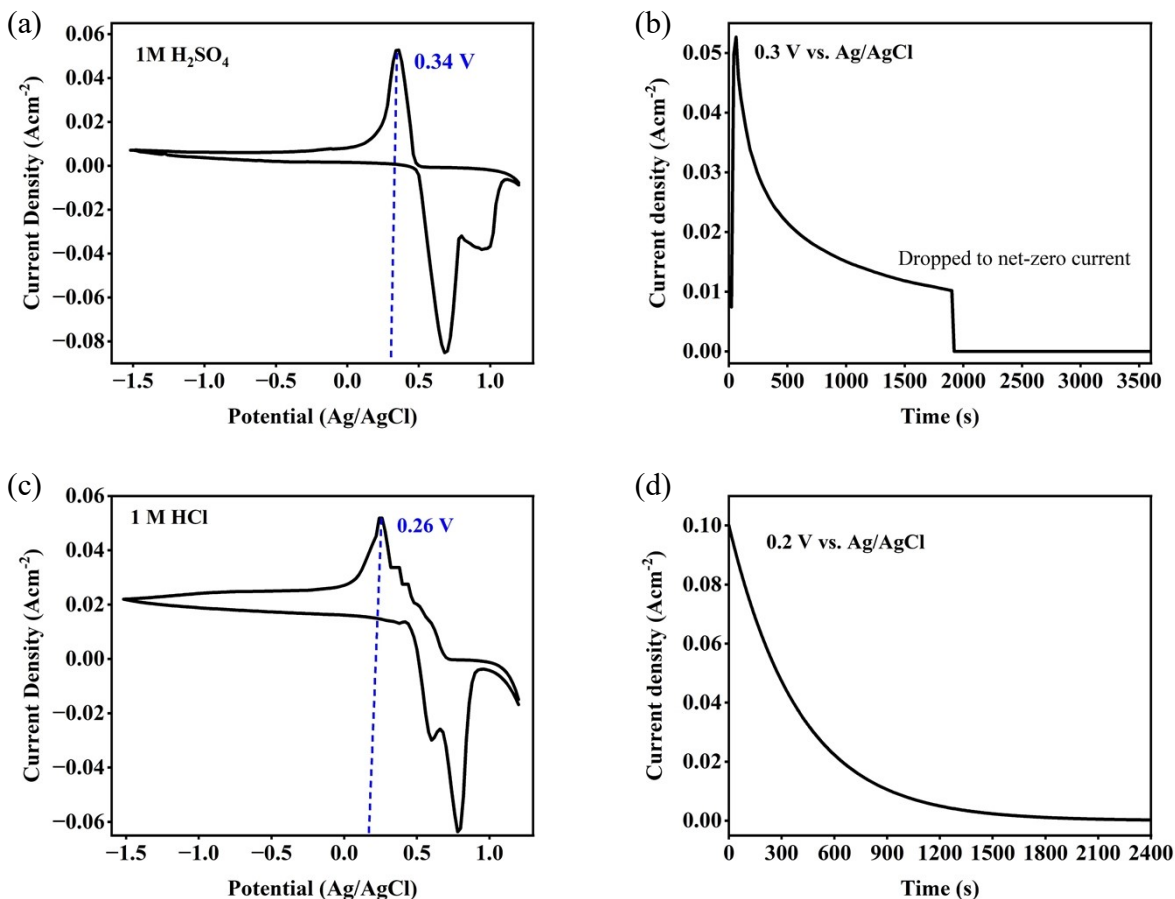


**Figure S1.** Preparation of electrodes using dealloying/etching method (a) Cyclic voltammogram of Bi<sub>50</sub>Pb<sub>40</sub>Sn<sub>10</sub> alloy foil obtained in 1 M H<sub>2</sub>SO<sub>4</sub> (b) chronoamperometric graph of Bi<sub>50</sub>Pb<sub>40</sub>Sn<sub>10</sub> alloy foil taken in 1 M H<sub>2</sub>SO<sub>4</sub> at controlled potential of 0.3 V (vs. Ag/AgCl). (c) Cyclic voltammogram of Bi<sub>50</sub>Pb<sub>40</sub>Sn<sub>10</sub> alloy foil obtained in 1 M HCl (d) chronoamperometric graph of Bi<sub>50</sub>Pb<sub>40</sub>Sn<sub>10</sub> alloy foil taken in 1 M H<sub>2</sub>SO<sub>4</sub> at controlled potential of 0.2 V (vs. Ag/AgCl).

## Mechanism of Sn and Pb Dissolution in acidic environment

### Reaction mechanism

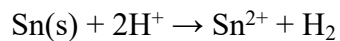
In an acidic medium (HCl, H<sub>2</sub>SO<sub>4</sub>), Sn oxidize to form Sn<sup>2+</sup> ions.



The electrons liberated in this oxidation are absorbed by  $H^+$  from  $HCl$  to produce hydrogen gas:



Overall reaction:



The dissolution of  $Pb$  in  $H_2SO_4$  undergo oxidation from  $Pb^0$  to  $Pb^{2+}$ , as listed by the following reaction:



**Table S1.** The contents of  $Pb$ ,  $Bi$ , and  $Sn$  elements in  $Bi_{50}Pb_{40}Sn_{10}$  alloy foil, Flaky  $Bi_{60}Pb_{40}$ , and web-like  $Bi_{85}Pb_{15}$  were determined by ICP-OES, respectively.

Elemental content	Weight (%)		
	Bi	Pb	Sn
$Bi_{50}Pb_{40}Sn_{10}$	<b>50.8</b>	<b>39.9</b>	<b>9.8</b>
$Bi_{60}Pb_{40}$ ,	<b>59.0</b>	<b>41.6</b>	-
$Bi_{85}Pb_{15}$	<b>85.7</b>	<b>16.3</b>	-

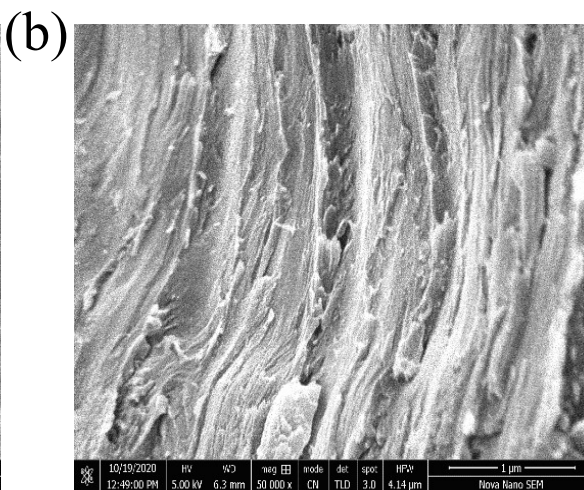
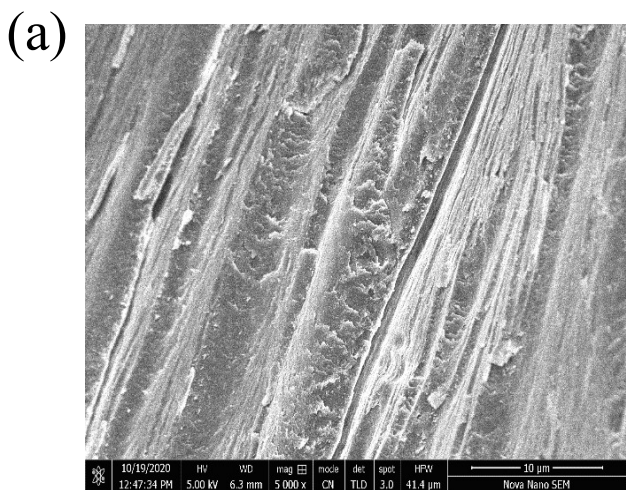


**Figure S2.** SEM mages of Bi<sub>50</sub>Pb<sub>40</sub>Sn<sub>10</sub> alloy foil at various magnifications.

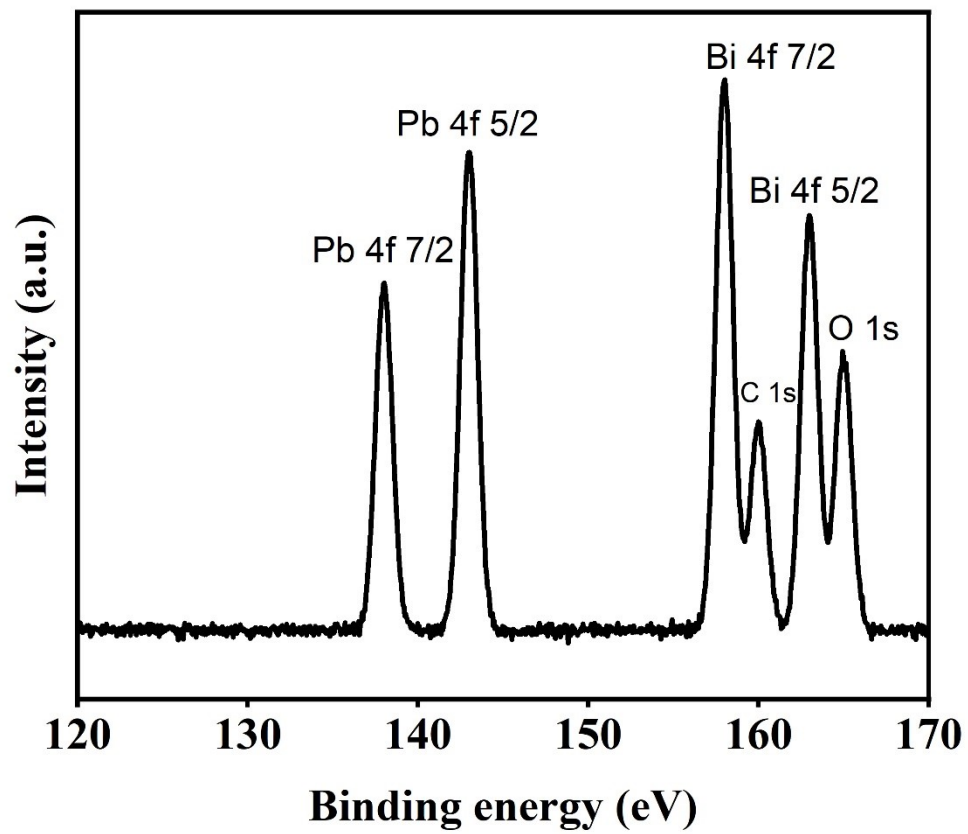


**Figure S3.** Overall XPS spectrum of Bi-Pb bimetallic alloy.

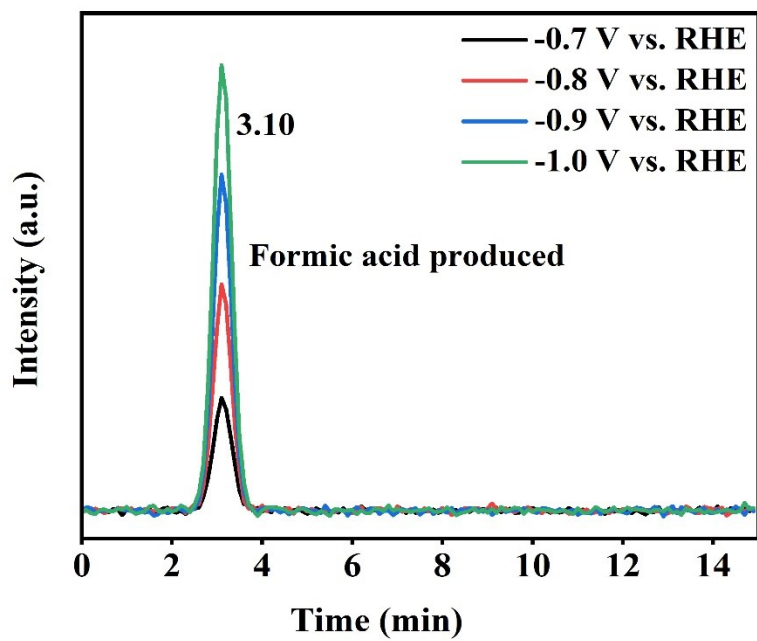


**Figure S4.** HPLC quantification of generated formic acid during CO<sub>2</sub> reduction reaction at different applied potentials.

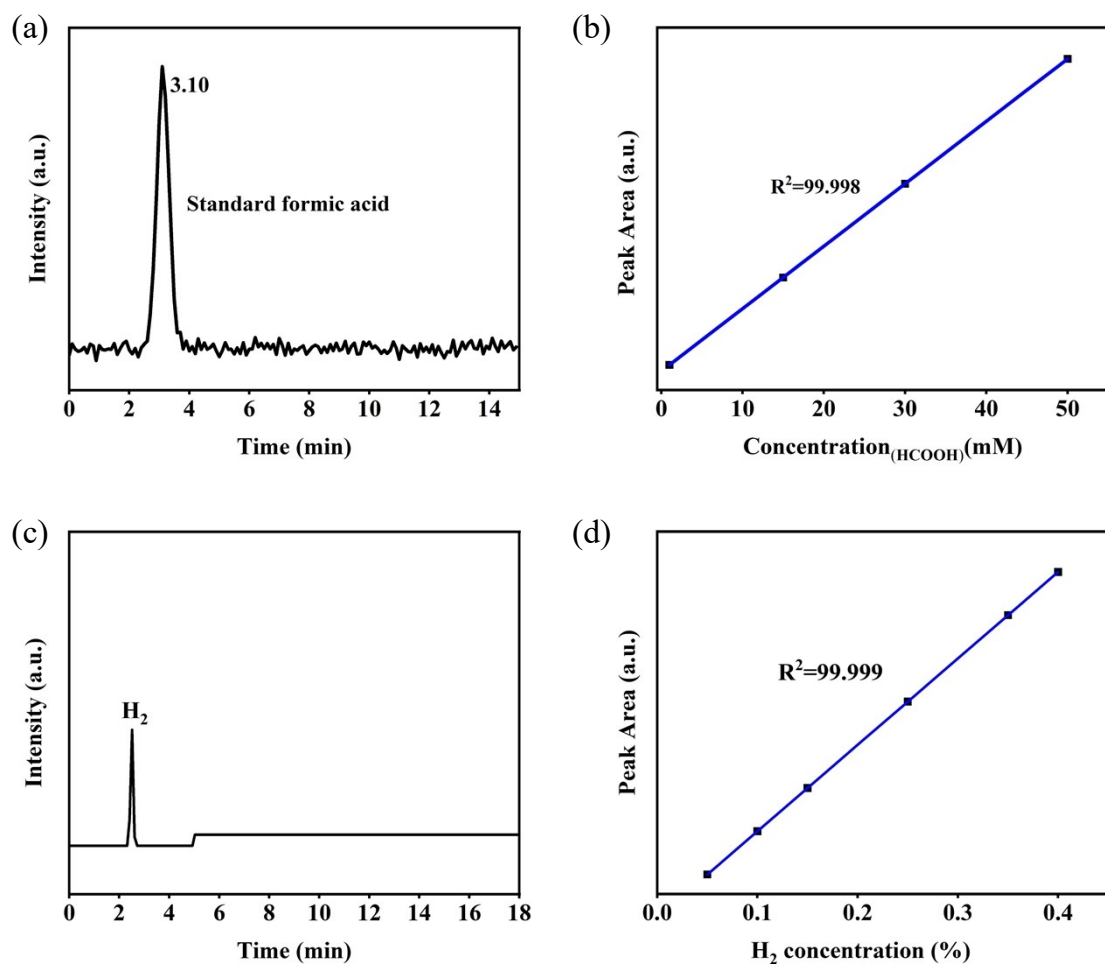


**Figure S5.** (a) Standard of commercial sodium formate (b) standard calibration curve between commercial sodium formate and corresponding peak area of HPLC at various concentration (c) Standard of hydrogen gas generated during reaction (d) standard calibration curve at various concentration.

The partial current density are calculated fom formate faradic efficiency and geometric current density as given below.

$$J_i = J_{\text{geometirc}} \times F.E \quad (2)$$

**Table S2.** Calculation of  $J_{\text{HCOOH}}$  of Flaky  $\text{Bi}_{60}\text{Pb}_{40}$ , Web-like  $\text{Bi}_{85}\text{Pb}_{15}$  and  $\text{Bi}_{50}\text{Pb}_{40}\text{Sn}_{10}$  alloy foil at various applied potentials from geometric current densities,  $FE_{\text{HCOOH}}$  respectively.

Potential (RHE)	Geometric current density ( $\text{mA cm}^{-2}$ )	$FE_{\text{CO}}$ (%)	$J_{\text{HCOOH}}$ ( $\text{mA cm}^{-2}$ )
Web-like $\text{Bi}_{85}\text{Pb}_{15}$			
-0.6	3.33954	36	1.20
-0.7	6.09741	55	3.35
-0.8	9.10339	69.8	6.35
-0.9	11.22437	81.3	9.12
-1.0	15	96.5	14.4
Flaky $\text{Bi}_{60}\text{Pb}_{40}$			
-0.6	2.60956	21	0.54
-0.7	4.18091	39	1.63
-0.8	7.12585	51	3.63
-0.9	8.18176	67	5.48
-1.0	9.43	83	7.82
$\text{Bi}_{50}\text{Pb}_{40}\text{Sn}_{10}$ alloy foil			
-0.6	1.41907	8	0.11
-0.7	3.33954	16	0.53
-0.8	4.62341	22	1.02
-0.9	5.59082	35	1.96
-1.0	6.09741	44	2.68

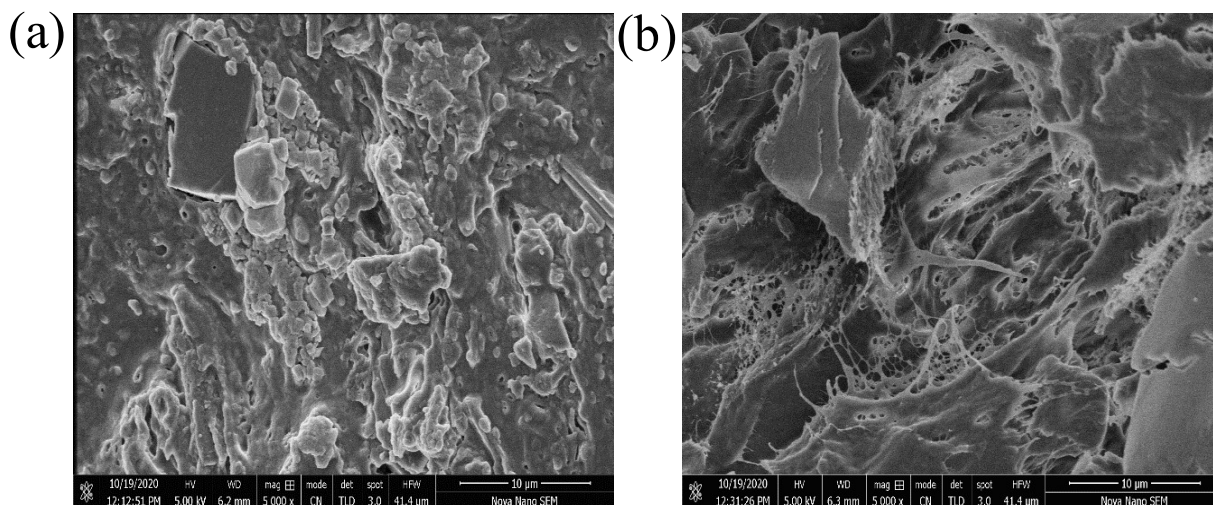


**Figure S6.** SEM images of prepared samples after CO<sub>2</sub> reduction electrolysis (a) Flaky Bi<sub>60</sub>Pb<sub>40</sub> (b) Web-like Bi<sub>85</sub>Pb<sub>15</sub>

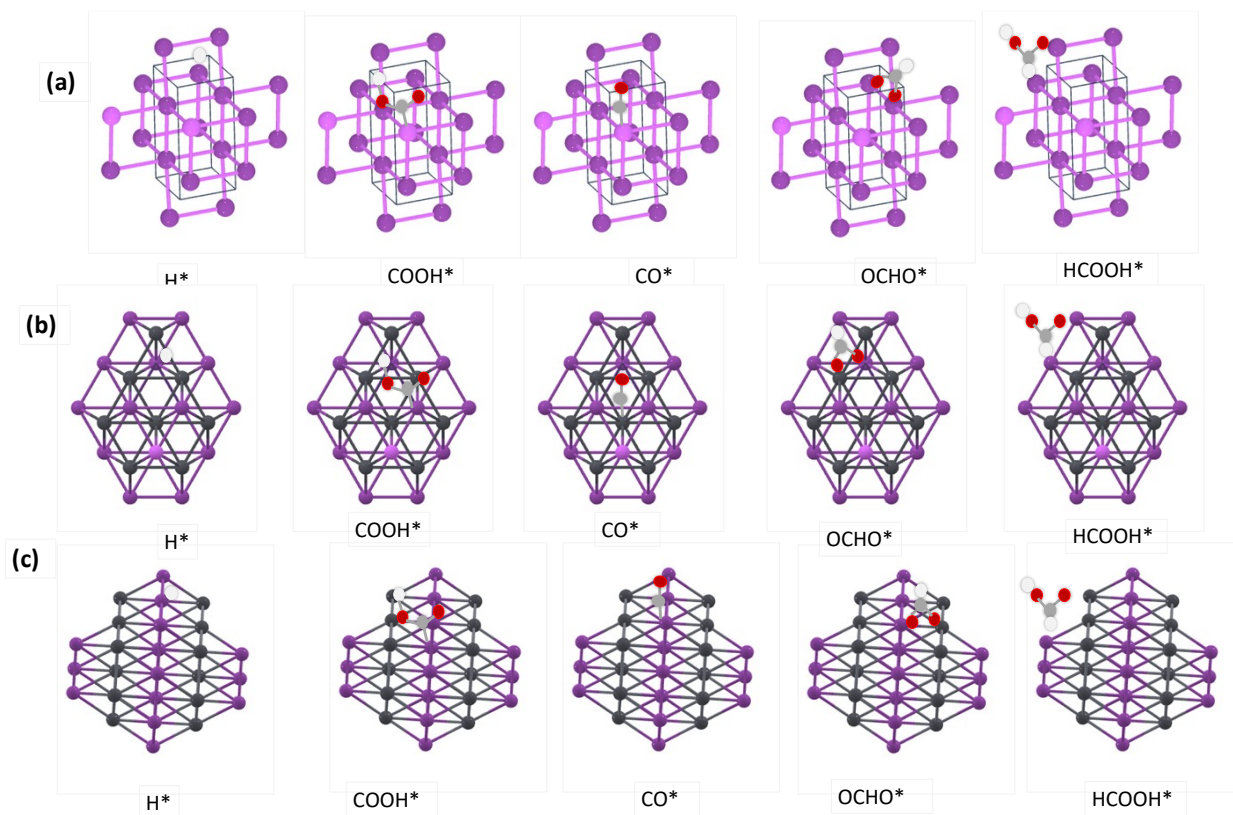


**Figure S7.** DFT optimized geometric models for surface slabs with adsorbed H\*, COOH\*, CO\*, OCHO\*, and HCOOH\* on (a) Bi<sub>100</sub>Pb<sub>0</sub> (b) Bi<sub>60</sub>Pb<sub>40</sub> (c) Bi<sub>85</sub>Pb<sub>15</sub> electrode surface as indicated; the purple, black, red, brown, and white circles characterize Bi, Pb, O, C, and H atoms, respectively.

**Table S3.** Comparison of charge transfer ( $R_{ct}$ ), solution resistance ( $R_s$ ) and phase constant element (CPE  $Y_0$ ,  $N$ ) of all samples.

Catalysts	$R_s$ ( $\Omega$ )		$R_{ct}$ ( $\Omega$ )		CPE ( $\mu\text{Mho} \cdot \text{s}^N$ )			$\chi^2$
	R	EE (%)	R	EE (%)	$Y_0$	N	EE (%)	
$\text{Bi}_{85}\text{Pb}_{15}$	38.323	2.4506	228.28	1.6207	0.00014256	0.76358	0.38567	0.00067
$\text{Bi}_{60}\text{Pb}_{40}$	39.06	2.0914	457.7	1.5252	0.00010043	0.80051	0.31288	0.000855
$\text{Bi}_{50}\text{Pb}_{40}\text{Sn}_{10}$	41.197	3.2589	4796.8	3.9898	6.6769E-05	0.80337	0.62019	0.00563

Here,  $R_s$  (Solution Resistance): Demonstrate the resistance of the electrolyte.  $R_{ct}$  (Charge Transfer Resistance): Reveals the resistance related with electron transfer at the electrode/electrolyte interface. CPE (Constant Phase Element): Shows the double-layer capacitance considering surface heterogeneity. EE (estimated error).

**Table S4.** For the  $\text{Bi}_{100}\text{Pb}_0(111)$ ,  $\text{Bi}_{85}\text{Pb}_{15}(111)$ , and  $\text{Bi}_{60}\text{Pb}_{40}(111)$  surfaces, reaction free energy (the values of  $\Delta E$ ,  $\Delta ZPE$ ,  $\Delta \int \text{CpdT}$ , and  $-\Delta TS$  in the four basic reaction steps of  $\text{CO}_2$  reduction) were calculated ( $U = 0$ ). All data is expressed in eV.

Elemental step*	$\Delta E$ (ev)	$\Delta ZPE$ (ev)	$\Delta \int \text{CpdT}$ (ev)	$-\Delta TS$ (ev)	$\Delta G$ (ev)
$\text{Bi}_{100}\text{Pb}_0(111)$					
(1)	0.07	0.00	-0.02	0.52	0.61
(2)	-0.19	0.20	-0.05	0.21	0.13
(3)	-0.10	0.23	-0.04	0.13	0.21
(4)	0.04	-0.06	-0.02	-0.81	-0.83
$\text{Bi}_{85}\text{Pb}_{15}(111)$					
(1)	0.07	0.00	-0.02	0.52	0.59
(2)	-0.61	0.20	-0.05	0.21	-0.24
(3)	0.19	0.23	-0.04	0.21	0.63
(4)	0.03	-0.06	-0.02	-0.82	-0.85
$\text{Bi}_{60}\text{Pb}_{40}(111)$					
(1)	0.00	0.00	-0.02	0.52	0.53
(2)	-0.73	0.20	-0.05	0.21	-0.35
(3)	0.33	0.20	-0.03	0.11	0.61
(4)	0.07	-0.06	-0.02	-0.82	-0.82

\*As stated in the main text's "Theoretical computations and mechanism discussion" section, it shows the basic elementary steps for  $\text{CO}_2$ -to- $\text{HCOOH}$  reduction.

The computational hydrogen electrode (CHE) model was used to compute the reaction free energies. Every stage of the electrochemical process was viewed as a simultaneous proton-electron

pair transfer that depended on the applied voltage. The following formulas provided the reaction free energy for stages 1 through 4:

$$\Delta G_{(1)} = G[*CO_2] - G[*] - G[CO_2] \quad (1)$$

$$\Delta G_{(2)} = G[*OCHO] - G[*CO_2] - G[H^+ + e^-] \quad (2)$$

$$\Delta G_{(3)} = G[*HCOOH] - G[*OCHO] - G[H^+ + e^-] \quad (3)$$

$$\Delta G_{(4)} = G[*] + G[HCOOH] - G[*HCOOH] \quad (4)$$

$$G[H^+ + e^-] = \frac{1}{2} G[H_2] - eU \quad (5)$$

where the elementary charge is denoted by “e” and the applied overpotential (against RHE) by “U”.

The following formula was used to determine all species' free energy:

$$G = E_{elec} + E_{ZPE} + \int C_p dT - TS \quad (6)$$

Where, ( $E_{elec}$ ) was the DFT-optimized total energy, zero-point energy ( $E_{ZPE}$ ), heat capacity ( $C_p$ ), and entropy (S). The latter quantities were computed using statistical mechanics within the harmonic approximation.

The following formula was then used to determine the binding energy ( $E_b$ ):

$$E_b = E_{ads/sub} - (E_{sub} + E_{ads}) \quad (7)$$

The total energies of the adsorbate-substrate system, the pristine surface, and the isolated adsorbate were denoted as  $E_{ads/sub}$ ,  $E_{sub}$ , and  $E_{ads}$ , respectively.

**Table S5.** The DFT-calculated binding energies ( $E_b$  in eV) for the \*OCHO and \*HCOOH intermediates on the  $Bi_{100}Pb_0(111)$ ,  $Bi_{85}Pb_{15}(111)$ ,  $Bi_{60}Pb_{40}(111)$  surfaces are presented, respectively.

Catalysts	$E_b$ (*OCHO)	$E_b$ (*HCOOH)
$Bi_{100}Pb_0(111)$	-2.73	-0.04
$Bi_{85}Pb_{15}(111)$	-3.14	-0.03
$Bi_{60}Pb_{40}(111)$	-3.26	-0.07

**Table S6.** Comparison of HCOOH selective CO<sub>2</sub> reduction catalysts in KHCO<sub>3</sub> electrolyte reported in literature.

Catalysts	Electrolyte	Potential	FE <sub>HCOOH</sub> (%)	Current density (mA cm <sup>-2</sup> )	Stability (hr.)	References
Web-like Bi <sub>85</sub> Pb <sub>15</sub>	0.2 M KHCO <sub>3</sub>	-1.0 V vs. RHE	96.5%	16	13	This work
Flaky Bi <sub>60</sub> Pb <sub>40</sub>	0.2 M KHCO <sub>3</sub>	-1.0 V vs. RHE	83%	9	13	
np-Bi	0.1 M KHCO <sub>3</sub>	-0.956 V vs. RHE	92.6%	14.2	24	1
Pb <sub>7</sub> Bi <sub>3</sub>	0.5 M KHCO <sub>3</sub>	-1.01 V vs. RHE	~91.86 %	15.56	-	2
In <sub>16</sub> Bi <sub>84</sub> NS (nanosphere)	0.5 M KHCO <sub>3</sub>	-0.94 V vs RHE	90%	14.1	-	3
Bi <sub>5</sub> Sn <sub>60</sub>	0.1 M KHCO <sub>3</sub>	-1.0 V vs. RHE	94.8%	34	20	4
Bi-Sn aerogel	0.1 M KHCO <sub>3</sub>	-1.0 V vs. RHE	93.9%	9.3	10	5
Cu-Bi	0.1 M KHCO <sub>3</sub>	-0.8 V vs. RHE	90%	>2	-	6
CuBi-100	0.5 M KHCO <sub>3</sub>	1.0 V vs. RHE	94.7%	12.8	8	7
BiIn <sub>5</sub> -500@C	0.5 M KHCO <sub>3</sub>	-0.86 V vs. RHE	97.5%	13.5	15	8
BixSny/Cu	0.1 M KHCO <sub>3</sub>	-0.84 (vs RHE)	90.4%	30	12	9
Cu <sub>1</sub> -Bi/Bi <sub>2</sub> O <sub>3</sub> @C	0.5 M KHCO <sub>3</sub>	-0.94 (vs RHE)	93.4%	10.1	10	10

## References

- [1] W. Lai, Y. Liu, M. Zeng, D. Han, M. Xiao, S. Wang, S. Ren and Y. J. N. Meng, *Nanomaterials* 2023, **13**, 1767.
- [2] X. Zhang, X. Jiao, Y. Mao, X. Zhu, H. Kang, Z. Song, X. Yan, X. Yan, C. Han, L. J. S. Cui, *Sep. Purif. Technol.* 2022, **300**, 121848.
- [3] D. Tan, W. Lee, Y. E. Kim, Y. N. Ko, M. H. Youn, Y. E. Jeon, J. Hong, J. E. Park, J. Seo, S. K. J. A. A. M. Jeong, *Appl. Mater. Interfaces* 2022, **14**, 28890-28899.
- [4] Z. Li, Y. Feng, Y. Li, X. Chen, N. Li, W. He and J. J. C. E. J. Liu, *Chem. Eng. J.* 2022, **428**, 130901.
- [5] Z. Wu, H. Wu, W. Cai, Z. Wen, B. Jia, L. Wang, W. Jin and T. J. A. C. Ma, *Angew. Chem. Int. Ed.* 2021, **133**, 12662-12667.
- [6] Z. B. Hoffman, T. S. Gray, Y. Xu, Q. Lin, T. B. Gunnoe and G. J. C. Zangari, *ChemSusChem.* 2019, **12**, 231-239.
- [7] Y. Xiong, B. Wei, M. Wu, B. Hu, F. Zhu, J. Hao and W. J. J. o. C. U. Shi, *J. CO<sub>2</sub> Util.* 2021, **51**, 101621.
- [8] Y. Guan, X. Zhang, Y. Zhang, T. N. Karsili, M. Fan, Y. Liu, B. Marchetti, X.-D. J. J. o. C. Zhou, *J. Colloid Interface Sci.* 2022, **612**, 235-245.
- [9] Q. Li, Y. Zhang, X. Zhang, H. Wang, Q. Li, J. Sheng, J. Yi, Y. Liu, and J. J. I. Zhang, *Ind. Eng. Chem. Res.* 2019, **59**, 6806-6814.
- [10] Y. Xue, C. Li, X. Zhou, Z. Kuang, W. Zhao, Q. Zhang and H. J. C. Chen, *ChemElectroChem.* 2022, **9**, e202101648.